NANO LETTERS

Letter

HPSTAR 167-2015

pubs.acs.org/NanoLett

Interfacial Effects on Lithium Superoxide Disproportionation in Li-O_2 Batteries

Dengyun Zhai,[†] Kah Chun Lau,[‡] Hsien-Hau Wang,[‡] Jianguo Wen,[§] Dean J. Miller,[§] Jun Lu,*[,†] Feiyu Kang,[∥] Baohua Li,[∥] Wenge Yang,[⊥] Jing Gao,[#] Ernesto Indacochea,[#] Larry A. Curtiss,*[,‡] and Khalil Amine*[,†]

[†]Chemical Sciences and Engineering Division, [‡]Materials Science Division, and [§]Electron Microscopy Center, Argonne National Laboratory, Argonne, Illinois 60439, United States

[∥]Engineering Laboratory for Next Generation Power and Energy Storage Batteries, Graduate School at Shenzhen, Tsinghua University, Shenzhen 518055, China

[⊥]High Pressure Synergetic Consortium, Geophysical Laboratory, Carnegie Institution of Washington, Argonne, Illinois 60439, United States

[#]Department of Civil and Materials Engineering, University of Illinois at Chicago, Chicago 60607, United States

S *Supporting Information*

ABSTRACT: During the cycling of Li-O_2 batteries the discharge process gives rise to dynamically evolving agglomerates composed of lithium−oxygen nanostructures; however, little is known about their composition. In this paper, we present results for a Li-O_2 battery based on an activated carbon cathode that indicate interfacial effects can suppress disproportionation of a LiO_2 component in the discharge product. High-intensity X-ray diffraction and transmission electron microscopy measurements are first used to show that there is a LiO_2 component along with Li_2O_2 in the discharge product. The stability of the discharge product was then probed by investigating the dependence of the charge potential and Raman intensity of the superoxide peak with time. The results indicate that the LiO_2 component can be stable for possibly up to days when an electrolyte is left on the surface of the discharged cathode. Density functional calculations on amorphous LiO_2 reveal that the disproportionation process will be slower at an electrolyte/LiO_2 interface compared to a vacuum/LiO_2 interface. The combined experimental and theoretical results provide new insight into how interfacial effects can stabilize LiO_2 and suggest that these interfacial effects may play an important role in the charge and discharge chemistries of a Li−O_2 battery.

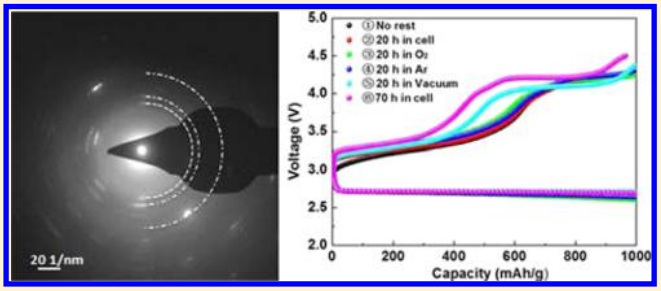

KEYWORDS: *Lithium−oxygen battery, lithium superoxide, stability, nanostructure, interface*

Among the possible alkali metal superoxides (MO_2), the superoxides of sodium, potassium, rubidium, and cesium (M = Na, K, Rb, and Cs) are known to exist in pure state, but not lithium (LiO_2).[1] Potassium superoxide is used for CO_2 absorption and regeneration of oxygen in spacecraft, submarine, and for fire fighters. Alkali metal superoxides are also interesting due to their intrinsic spin one-half state and the presence of complex magnetic properties including paramagnetic, antiferromagnetic, and spin-flop phases.[2] These magnetic phase transitions are also related to intricate structural phase transformations at low temperatures due to increased O_2^- anion ordering and hindered rotation upon cooling.[1] Recently, there has also been interest in sodium and potassium superoxide for batteries.[3,4]

In contrast, LiO_2 has never been shown to exist in pure state at room temperature.[5] The LiO_2 molecule has been prepared by matrix isolation at 4 K and characterized with use of an electron spin resonance (ESR) technique.[6] A few attempts to synthesize solid LiO_2 have been carried out. One approach involving direct oxidation of Li metal in oxygen-saturated liquid ammonia suggested the presence of LiO_2 at −78 °C, but it was not isolated.[7] Treatment of Li_2O_2 with ozone dissolved in Freon-12 at −65 °C was also reported to result in a mixture of LiO_2 and Li_2O_2,[8,9] but again the LiO_2 was not isolated.

Despite the lack of evidence for LiO_2 being stable under ambient conditions, several research groups have reported evidence for LiO_2-like species in the discharge product in a Li-O_2 battery.[10−14] This may result from LiO_2 being a possible reaction species in the discharge mechanism for Li-O_2 batteries.[15−20] The discharge mechanism for the Li-O_2 cell is believed by some researchers to be a two-electron transfer step (eq 1) in the discharge half-cycle (aprotic cell, net reaction)[20,21]

$$2Li^+ + 2e^- + O_2 \rightarrow Li_2O_2 \quad (1)$$

Received: October 13, 2014
Revised: December 26, 2014
Published: January 23, 2015

DOI: 10.1021/nl503943z
Nano Lett. 2015, 15, 1041−1046

The first step of an oxygen reduction reaction (ORR) involves LiO_2 formation (eqs 2 and 3)[21,22]

$$O_2 + 1e^- \rightarrow O_2^- \quad (2)$$

$$O_2^- + Li^+ \rightarrow LiO_2 \quad (3)$$

Alternatively, a disproportionation reaction could also generate Li_2O_2 from LiO_2 (eq 4)

$$2LiO_2 \rightarrow Li_2O_2 + O_2 \quad (4)$$

Thus, LiO_2 could be present in the discharge product if disproportionation is slow enough, which suggests the possibility of the stability of LiO_2 at room temperature.

Our recent studies based on a high surface area activated carbon (AC) cathode in a Li−O_2 battery have given discharge products composed of toroidal assemblies of lithium−oxygen nanostructures. We have identified a LiO_2-like species in the toroids based on Raman and magnetic measurements.[14] In addition, a kinetics analysis of charge plateaus is consistent with a disproportionation reaction [eq 4] with first order kinetics that generates Li_2O_2 from LiO_2.[13] The AC apparently results in nucleation and growth of a discharge product with these two components and is also reflected in the two plateaus (3.0−3.5 and 4.0−4.5 V) observed for the charge potential. Our recent experimental[12] and theoretical[23] results have provided evidence that a slow disproportionation results in a discharge product with some LiO_2 present.

Although the previous studies provided evidence that some type of LiO_2-like component can be present in the LiO_2-battery discharge product, it is desirable to obtain a better understanding of the nature of this component, as it could play a key role in reducing the charge overpotentials in these batteries. Herein, we present new experimental results on the nature of the LiO_2-like component by use of synchrotron X-ray high-resolution X-ray diffraction (XRD), electron microscopy, and electron diffraction that indicate the presence of some crystalline LiO_2 in the Li−O_2 discharge product based on recently predicted LiO_2 crystal structure.[24,25] The LiO_2 was found to be surprisingly stable using Raman spectroscopy and electrochemical analysis under various environments, which can be attributed to an interfacial effect that slows disproportionation.

Evidence for Composition of Discharge Product. In this work, the discharged AC electrode was examined by high-energy XRD, as shown in Figure 1. Three distinct peaks are identified as the (100), (101), and (110) peaks of Li_2O_2 according to the standard XRD histogram of Li_2O_2 (JCPDS No. 09-0355). There are several weaker peaks marked with an asterisk "*" that do not match with Li_2O_2 or other possible products from side reactions such as LiOH or Li_2CO_3. Interestingly, these XRD peaks are consistent with the XRD pattern of a LiO_2 crystalline phase based on theoretical study by Lau et al.,[25] although the relative intensities do not match perfectly. There is no evidence for other possible decomposition species such as LiOH and Li_2CO_3 observed in the XRD data. In addition, no evidence for LiOH or Li_2CO_3 is found in the Raman spectra (Figure 4, below) or in the Fourier transfer infrared (FTIR) spectra (Figure S1 in the Supporting Information). On the basis of these results, the XRD data suggests at least some of the LiO_2-like species has a structure similar to that predicted for a LiO_2 crystalline structure. According to previous kinetic analysis the proportion of the LiO_2-like component on the discharged AC is probably close to

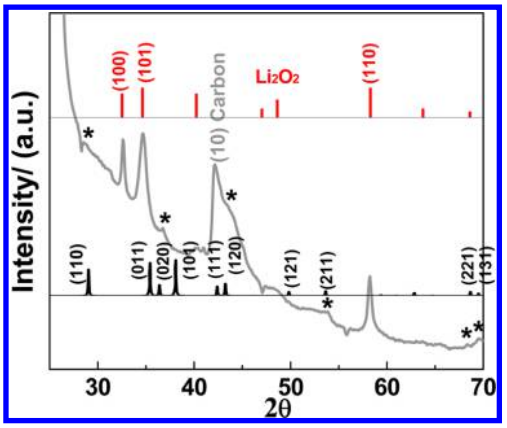

Figure 1. XRD pattern of the discharged AC cathode for 1000 mAh/g with a current density of 0.2 mA/cm^2. The weak peaks that are consistent with the calculated LiO_2 Bragg peaks are marked with asterisk "*". The red histogram corresponds to the standard Li_2O_2 patterns. The LiO_2 pattern (black histogram) is from the structure calculated from density functional theory.[25] (For comparison with our previous studies,[12,13] the XRD data of the discharged electrode was converted from being based on a wavelength of 0.11165 to 1.54 Å).

~50% (Figure S2 in the Supporting Information). Because there are only a few weak crystalline LiO_2 XRD peaks it is reasonable to assume that the remainder of the LiO_2-like component may be amorphous or in a disordered phase, instead of a crystalline form. The "LiO_2-like" term was used to include the possibility for partial or incomplete disproportionation corresponding to an oxygen-rich Li_xO_y stoichiometry (i.e., $x < y$) other than LiO_2.[12]

The toroids on the discharged AC electrode were also probed by transmission electron microscopy (TEM). Figure 2a−c shows TEM images of the toroids, which are similar to the morphologies of toroids observed by scanning electron microscopy (SEM) (Figure S3 in the Supporting Information). Areas located on the outer parts of the toroid were probed by selected area electron diffraction (SAED) (Figure S4 in the Supporting Information). For most areas examined, the electron diffraction patterns exhibit broad and diffuse rings, as shown in Figure 2d, which indicate the components in those areas are amorphous. However, for some areas diffraction patterns with discrete reflections are observed as in Figure 2e, indicating that material in these selected areas are crystalline. The reflections in these patterns correspond to lattice spacings of 3.08, 2.60, 1.88 Å, which do not match Li_2O_2, but are consistent with LiO_2 lattice planes (1,−1,0), (0,1,−1) and (1,−2,1), as shown in Figure 2f. This data suggests there is some crystalline LiO_2 present in the discharge product, consistent with the XRD data. The Li_2O_2 component is also identified in results shown in Figure 2. Our previous studies indicated that the LiO_2 component may decompose at a lower charge voltage of 3.0−3.5 V and Li_2O_2 may decompose at higher charge voltage above ~4.0 V.[13] The discharged cathode was then charged back to 3.5 V (Figure S5 in the Supporting Information) and the toroids on the cathode were probed by SEM and TEM imaging, as shown in Figure 2g and Figure S6 in the Supporting Information.The nanostructured surface texture of toroids becomes more pronounced after LiO_2 component decomposes. The SAED pattern of the toroid in Figure 2g is consistent with Li_2O_2, as shown in Figure 2h. This is consistent with previous results from Raman[12] and magnetic[14] data that

DOI: 10.1021/nl503943z
Nano Lett. 2015, 15, 1041−1046

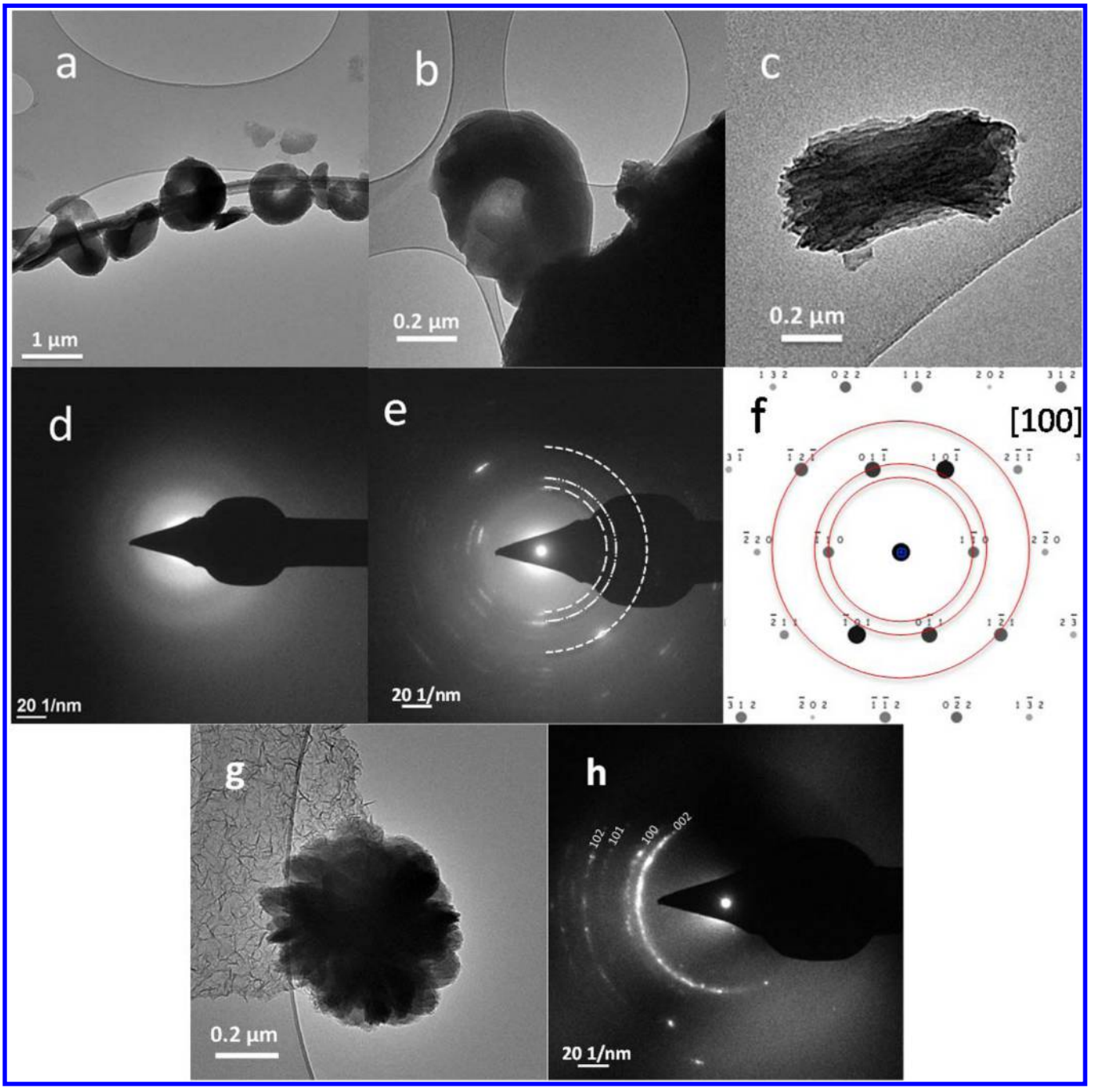

Figure 2. (a–c) TEM images of toroids from discharged AC electrode for 1000 mAh/g at 0.2 mA/cm^2; (d,e) SAED patterns on edge of the toroid; (f) simulated SAED patterns for LiO_2 [100];[25] (g) TEM image of toroid from AC electrode that is first discharged for 1000 mAh/g at 0.2 mA/cm^2 and then charged back to 3.5 V at 0.1 mAh/cm^2; (h) SAED pattern of toroid in panel g showing Li_2O_2.

show no evidence for an LiO_2 component when charged back to 3.5 V.

Thus, the above XRD and TEM results give direct evidence for some LiO_2 being present in the LiO_2-battery discharge product along with Li_2O_2. The high energy XRD shows characteristic LiO_2 peaks that were not found using conventional XRD equipment in the previous work.[13,14] The presence of LiO_2 is further supported by electron diffraction. Although previous kinetics analysis[13] indicates that a significant fraction (~40–50%) has not yet undergone disproportionation, the weakness of the peaks suggests that much of the LiO_2 might possibly be amorphous or some other oxygen rich Li_xO_y stoichiometry, which is also consistent with observations by electron microscopy and diffraction.

Dependence of Disproportionation on the Nature of the LiO_2 Interface. The stability of the discharge product from the AC-based Li-O_2 cell was further investigated by varying the interface conditions of the discharge product and characterizing the subsequent effect on the disproportionation process with time. Six different conditions were investigated with the resulting charge curves given in Figure 3:

1. The cell in the glass chamber is filled with O_2 (i.e., no rest between discharge and charge cycle).

DOI: 10.1021/nl503943z
Nano Lett. 2015, 15, 1041–1046

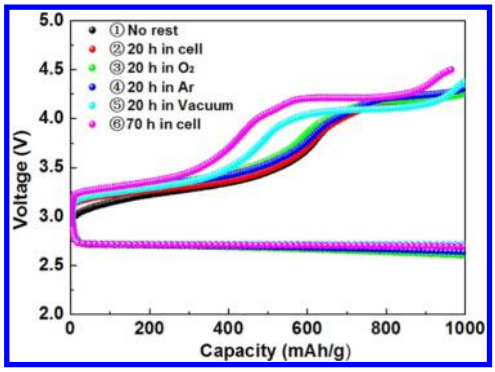

Figure 3. Galvanostatic discharge/charge curves of cells under the six different conditions described in the text. The discharged capacity is 1000 mAh/g, and the discharge/charge current density is 0.2 and 0.1 mA/cm^2, respectively.

2. The cell after discharge was kept for 20 h in the glass chamber filled with O_2.

3. The cell after discharge was disassembled and kept under O_2 for 20 h.

4. The cell after discharge was disassembled and kept under Ar for 20 h.

5. The cell after discharge was disassembled and the discharged electrode was kept under vacuum for 20 h.

6. The cell after discharge was kept for 70 h in the glass chamber filled with O_2.

Conditions #2−5 were done for 20 h and the condition #6 was done for 70 h. The electrolyte is kept in the cell except for #5 where it is under vacuum. In order to optimize the LiO_2 percentage, all six cells were discharged to 1000 mAh/g at a relatively high current density of 0.2 mA/cm^2. Then these six different cells were charged back to 1000 mAh/g at a lower current density of 0.1 mA/cm^2, and the voltage profiles are shown in Figure 3. From this figure, it can be seen that according to the procedure for the 20 h aging time (#2−4) the voltage profiles remain nearly unchanged from the cell with no aging time (#1, no rest).

Our previous studies have indicated the LiO_2 component may decompose at a lower charge voltage of 3.0−3.5 V and Li_2O_2 may decompose at higher charge voltage above ∼4.0 V.[13] Because the voltage profiles for the discharged cathode kept in the cell (#2), under O_2 (#3), and under Ar (#4) for 20 h remain similar to that of the cell with no rest (#1), it is reasonable to conclude that the LiO_2 component is stable (i.e., does not significantly disproportionate) for at least 20 h under these three interface conditions. When the discharged cathode was placed in vacuum for 20 h or in cell for 70 h (conditions #5 and 6), it is found that the proportion of LiO_2 in the product is decreasing based on the reduced ratio of lower charge voltage relative to the whole charge voltage profile, although some of LiO_2 component still remains. Thus, in a vacuum disproportionation proceeds at a faster rate and it becomes more apparent over a longer time period.

To further investigate the stability of the LiO_2 component in the discharge products under different interface conditions, the six discharged cathodes were characterized by Raman spectroscopy, as shown in Figure 4. The electrolyte is kept in the cell for the noted period of time after which it is dried with dimethyl carbonate (see Supporting Information). The Raman spectra from these six different discharged cathodes all have a peak at ∼1123 cm^{-1} (denoted as S1) associated with the

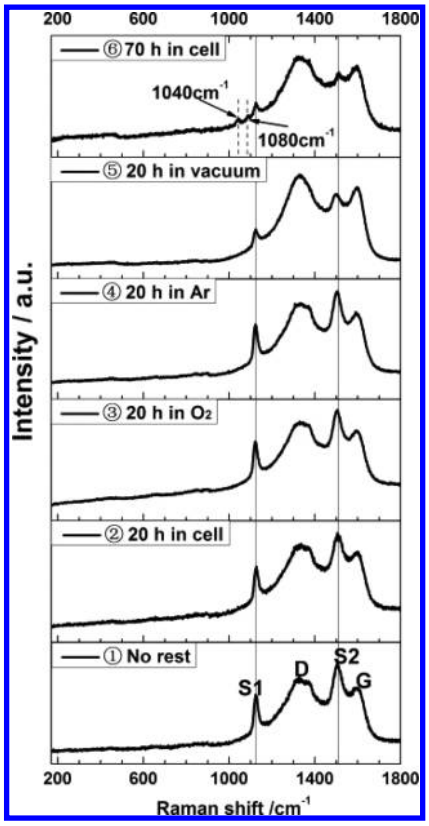

Figure 4. Raman spectra of the toroids on the surface of the discharged AC cathode for the six different conditions described in the text. The values of the peaks (in cm^{-1}) are 1123 (S1), 1505 (S2), 1340 (D), and 1600 (G).

presence of a LiO_2-like species in the toroids, which was identified in our previous work.[13,14] Another peak at ∼1505 cm^{-1} (denoted as S2) in the Raman spectra is due to the coupled interface between the LiO_2 component and the carbon electrode surface[12] and thus is another signature for the presence of LiO_2 component in the discharge product. For conditions #2−4, the relative intensity of Raman peaks S1 and S2 for the discharge product are found to be similar to that of the Raman spectra taken of the discharge product with no aging (#1). This suggests that the LiO_2 component has not significantly disproportionated further under the cell/O_2/Ar gas conditions for 20 h, which is consistent with the electrochemical results for these three conditions. In contrast for the discharged AC cathodes kept in vacuum for 20 h or in cell for 70 h, the intensity of peaks S1 and S2 becomes weaker relative to the Raman spectra taken of the discharge product with no aging (#1). This again further confirms that some of the LiO_2 component disproportionates when exposed to vacuum for 20 h or ages in the cell for 70 h.

Insight from Theory. In order to gain insight into this new experimental evidence for stability of LiO_2 during rest after discharge, we investigated the effect of the presence of an electrolyte on the stability of an amorphous LiO_2 surface using density functional theory (DFT) calculations. We have carried out calculations on an amorphous stoichiometric LiO_2 slab with a thickness of about 1.2 nm (Figure 5). From the computed radial distribution function (RDF) (see Figure S7 in the Supporting Information) of the optimized geometry of an amorphous LiO_2 slab, the dominant local atomic coordinations

DOI: 10.1021/nl503943z
Nano Lett. 2015, 15, 1041−1046

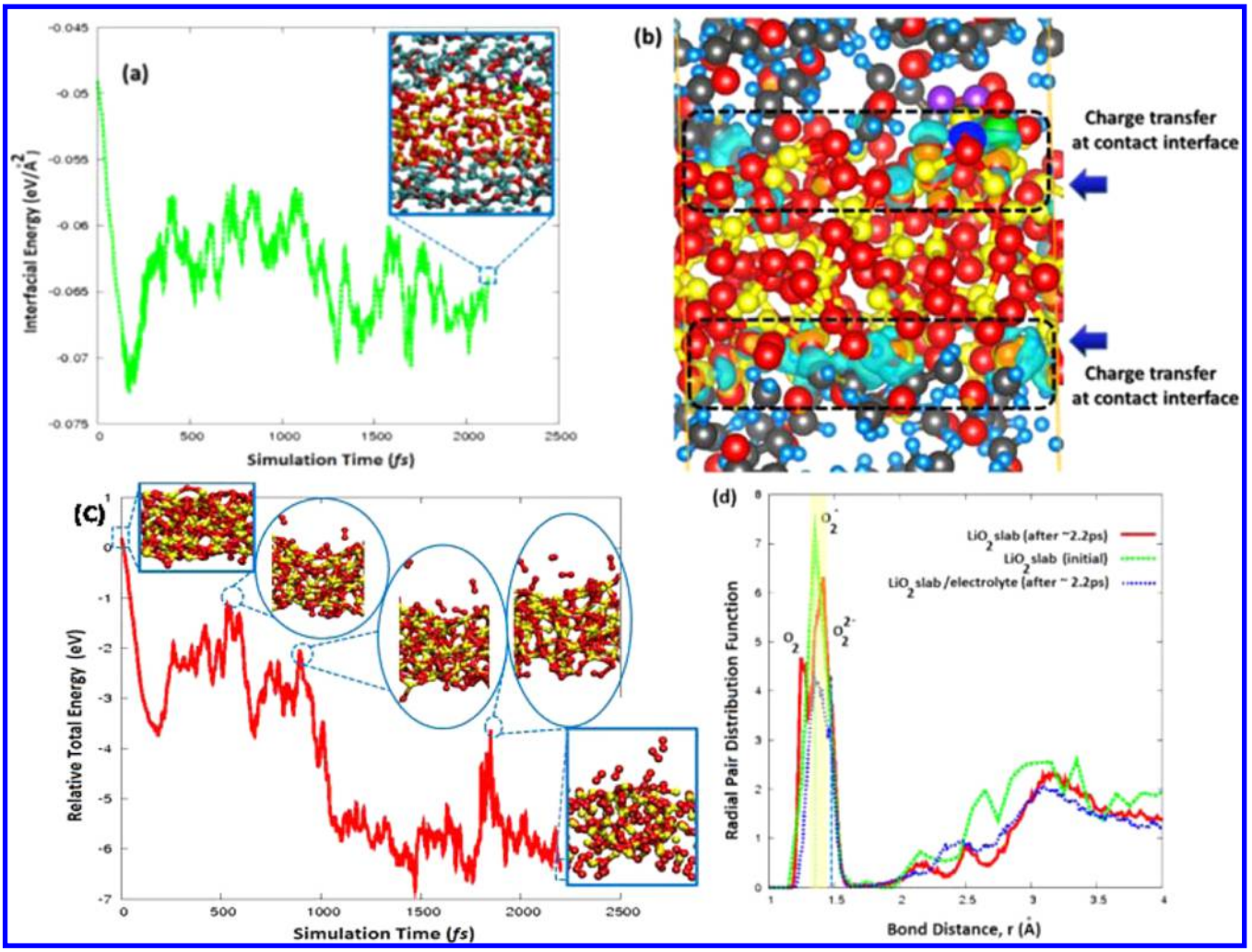

Figure 5. (a) An AIMD simulation of an amorphous LiO_2 slab/electrolyte interface at an equilibrium temperature of T = 300 K. (b) Charge transfer (light blue) at the LiO_2 slab/electrolyte interface from a charge density plot during a particular snapshot of a AIMD trajectrory. (c) The AIMD simulation of a bare amorphous LiO_2 slab exposed to vacuum with thermal equilibration at T = 300 K that shows the gradual thermal decomposition of outermost surface layer of LiO_2 through a thermally activated disproportionation reaction to release O_2 molecules. (d) Radial pair distribution function of a O−O pair (g_{O-O}) versus O−O bond distance (r_{O-O}) obtained from AIMD trajectories for an amorphous LiO_2 slab/electrolyte (after ~2.2 ps) together with g_{O-O} of amorphous LiO_2 slab (vacuum) initially and after an ~2.2 ps simulation run. The carbon, oxygen, lithium, sulfur, and fluorine atoms are in gray, red, yellow, green, and purple color, respectively.

of Li−O and O−O are found to be bulk like and similar to that predicted for crystalline bulk LiO_2.[25]

To study its interface with an electrolyte we have carried out ab initio molecular dynamics (AIMD) simulations at room temperature. From the thermal equilibration at T = 300 K for ~2.2 ps, it is found that the amorphous LiO_2 slab/electrolyte has an interfacial energy of ~−64.5 meV/Å^2 when thermal equilibrium is achieved (Figure 5a) after 1 ps simulation. Throughout the whole simulation, the amorphous LiO_2 slab is found to be quite stable with the outermost surface-bounded superoxide groups not coming off. As shown in Figure 5b, there is substantial charge transfer at the contact interface with electrolyte. In contrast to a bare amorphous LiO_2 surface exposed to vacuum (Figure 5c), the undercoordinated superoxide species are stabilized through interaction with the solvent and $LiCF_3SO_3$ molecules as shown in Figure 5b. The charge transfer observed in the AIMD simulation can be attributed to the interaction of surface superoxide species with methyl (CH_3) and methylene (CH_2) groups from the ether solvent and sometimes with a $LiCF_3SO_3$ salt molecule at the LiO_2 slab/electrolyte interface (Supporting Information Figure S8). Therefore, relative to the bare amorphous LiO_2 surface exposed to the vacuum, the disproportionation rate is expected to be slower when the LiO_2 surface is covered with an electrolyte. A qualitatively similar trend is found in the experimental observations where the discharge products covered by electrolyte (#2−4) show lack of evidence of disproportionation for at least 20 h. However, evaporation or the degradation of electrolyte may facilitate the disproportionation observed after 70 h.

To qualitatively correlate the decreasing Raman intensity S1 (Figure 4) of the superoxide species (~1123 cm^{-1}) to disproportionation of LiO_2, we turn to an analysis of the radial pair correlation function of the O−O bond (i.e., g_{O-O}) obtained from AIMD atomic trajectories. From the AIMD simulations, the desorption of O_2 and the formation of Li_2O_2 through the disproportionation of LiO_2 can be represented by the time-evolution of g_{O-O} shown in Figure 5d. If no disproportionation of LiO_2 is taking place, then the first sharp dominant peak of g_{O-O} within the first coordination shell of an LiO_2 amorphous

DOI: 10.1021/nl503943z
Nano Lett. 2015, 15, 1041−1046

slab will be exclusively represented as a superoxide species with bond distance $r_{O-O} \sim 1.3-1.4$ Å. This is shown in Figure 5d where after ~2.2 ps of AIMD simulation with electrolyte on the surface, the first dominant peak of g_{O-O} of the amorphous LiO_2 slab is exclusively superoxide species. In contrast for the bare amorphous LiO_2 slab exposed to vacuum, the dominant peak (Figure 5d) of g_{O-O} has a lower intensity and is significantly broadened. This broadened first peak can be represented by an oxygen molecule ($r_{O-O} \sim 1.23-1.25$ Å), a superoxide species ($r_{O-O} \sim 1.3-1.4$ Å) and a peroxide species ($r_{O-O} \sim 1.45-1.5$ Å) that corresponds to the disproportionation process of LiO_2. This can account for the decreased Raman intensity for the LiO_2 exposed to a vacuum.

In summary, the results for a Li-O_2 battery based on an AC cathode presented here provide evidence that interfacial effects can slow disproportionation of a LiO_2 component in the discharge product. Characterization of the discharge product by both high intensity XRD and TEM measurements reveals that there is a LiO_2 component along with Li_2O_2 in the product. The stability of the discharge product was probed by investigating the dependence of the charge potential and Raman intensity of the superoxide peak with over a time periods of 20 and 70 h. The results indicate that the LiO_2 component can be stable for possibly up to days when an electrolyte is left on the surface of the discharged cathode. The results are explained by DFT calculations on amorphous LiO_2 that find the disproportionation process to be slower at an electrolyte/LiO_2 interface compared to a vacuum/LiO_2 interface. The combined experimental and theoretical results provide new insight into how interfacial effects can stabilize LiO_2, which may play an important role in the charge and discharge chemistries of a Li-O_2 battery.

■ ASSOCIATED CONTENT

Supporting Information

Material synthesis, cell assembly and measurement, characterization, and modeling. This material is available free of charge via the Internet at http://pubs.acs.org.

■ AUTHOR INFORMATION

Corresponding Authors

*E-mail: junlu@anl.gov (J.L.).
*E-mail: curtiss@anl.gov (L.A.C.).
*E-mail: amine@anl.gov (K.A.).

Author Contributions

D.-Y.Z. and K.-C. L. contributed equally.

Notes

The authors declare no competing financial interest.

■ ACKNOWLEDGMENTS

This work was supported by the U.S. Department of Energy under Contract DE-AC02-06CH11357 from the Vehicle Technologies Office, Department of Energy, Office of Energy Efficiency and Renewable Energy (EERE). We also acknowledge grants of computer time through INCITE awards for BlueGene/Q computer at Argonne National Laboratory and allocations on the CNM Carbon Cluster at Argonne National Laboratory, the ALCF Fusion Cluster at Argonne National Laboratory, and the EMSL Chinook Cluster at Pacific Northwest National Laboratory. Use of the Advanced Photon Source, Center for Nanoscale Materials, and the Electron Microscopy Center for Materials Research was supported by the U.S. Department of Energy, Office of Science, Office of Basic Energy Sciences, under contract No. DE-AC02-06CH11357.

■ REFERENCES

(1) Hesse, W.; Jansen, M.; Schnick, W. *Prog. Solid State Chem.* **1989**, *19*, 47−110.
(2) Bosch, M. A.; Lines, M. E. *Phys. Rev. Lett.* **1980**, *45*, 140−143.
(3) Ren, X.; Wu, Y. *J. Am. Chem. Soc.* **2013**, *135*, 2923−2926.
(4) Hartmann, P.; Bender, C. L.; Vracar, M.; Durr, A. K.; Garsuch, A.; Janek, J.; Adelhelm, P. *Nat. Mater.* **2013**, *12*, 228−232.
(5) Sangster, J.; Pelton, A. D. *J. Phase Equilib.* **1992**, *13*, 296−299.
(6) Lindsay, D. M.; Garland, D. A. *J. Phys. Chem.* **1987**, *91*, 6158−6161.
(7) Thompson, J. K.; Kleinberg, J. *J. Am. Chem. Soc.* **1951**, *73*, 1243−1245.
(8) Bakulina, V. M.; Tokareva, S. A.; Vol'nov, I. I. *J. Struct. Chem.* **1967**, *8*, 980−981.
(9) Carter, G. F.; Templeton, D. H. *J. Am. Chem. Soc.* **1953**, *75*, 5247−5249.
(10) Adams, B. D.; Radtke, C.; Black, R.; Trudeau, M. L.; Zaghib, K.; Nazar, L. F. *Energy Environ. Sci.* **2013**, *6*, 1772−1778.
(11) Gallant, B. M.; Kwabi, D. G.; Mitchell, R. R.; Zhou, J.; Thompson, C. V.; Shao-Horn, Y. *Energy Environ. Sci.* **2013**, *6*, 2518−2528.
(12) Zhai, D.; Wang, H.-H.; Lau, K. C.; Gao, J.; Redfern, P. C.; Kang, F.; Li, B.; Indacochea, E.; Das, U.; Sun, H.-H.; Sun, H.-J.; Amine, K.; Curtiss, L. A. *J. Phys. Chem. Lett.* **2014**, *5*, 2705−2710.
(13) Zhai, D.; Wang, H. H.; Yang, J.; Lau, K. C.; Li, K.; Amine, K.; Curtiss, L. A. *J. Am. Chem. Soc.* **2013**, *135*, 15364−15372.
(14) Yang, J.; Zhai, D.; Wang, H. H.; Lau, K. C.; Schlueter, J. A.; Du, P.; Myers, D. J.; Sun, Y. K.; Curtiss, L. A.; Amine, K. *Phys. Chem. Chem. Phys.* **2013**, *15*, 3764−3771.
(15) Xu, J. J.; Wang, Z. L.; Xu, D.; Zhang, L. L.; Zhang, X. B. *Nat. Commun.* **2013**, *4*, 2438−2447.
(16) Ottakam Thotiyl, M. M.; Freunberger, S. A.; Peng, Z.; Chen, Y.; Liu, Z.; Bruce, P. G. *Nat. Mater.* **2013**, *12*, 1050−1056.
(17) Peng, Z.; Freunberger, S. A.; Chen, Y.; Bruce, P. G. *Science* **2012**, *337*, 563−566.
(18) Mitchell, R. R.; Gallant, B. M.; Thompson, C. V.; Shao-Horn, Y. *Energy Environ. Sci.* **2011**, *4*, 2952−2958.
(19) Abraham, K. M. *J. Electrochem. Soc.* **1996**, *143*, 1−5.
(20) Girishkumar, G.; McCloskey, B.; Luntz, A. C.; Swanson, S.; Wilcke, W. *J. Phys. Chem. Lett.* **2010**, *1*, 2193−2203.
(21) Peng, Z.; Freunberger, S. A.; Hardwick, L. J.; Chen, Y.; Giordani, V.; Barde, F.; Novak, P.; Graham, D.; Tarascon, J. M.; Bruce, P. G. *Angew. Chem., Int. Ed.* **2011**, *50*, 6351−6355.
(22) Laoire, C. O.; Mukerjee, S.; Abraham, K. M.; Plichta, E. J.; Hendrickson, M. A. *J. Phys. Chem. C* **2009**, *113*, 20127−20134.
(23) Das, U.; Lau, K. C.; Redfern, P. C.; Curtiss, L. A. *J. Phys. Chem. Lett.* **2014**, *5*, 813−819.
(24) Zhuravlev, Y. N.; Obolonskaya, O. S. *J. Struct. Chem.* **2010**, *51*, 1005−1013.
(25) Lau, K. C.; Curtiss, L. A.; Greeley, J. *J. Phys. Chem. C* **2011**, *115*, 23625−23633.

DOI: 10.1021/nl503943z
Nano Lett. 2015, 15, 1041−1046